

# Detection of low-energy protons using a silicon drift detector

M. Simson <sup>a,\*</sup>, P. Holl <sup>c,e</sup>, A.R. Müller <sup>a</sup>, A. Nicolae <sup>c,e</sup>, G. Petzoldt <sup>a</sup>, K. Schreckenbach <sup>b</sup>, H. Soltau <sup>c,e</sup>,  
L. Strüder <sup>d,e</sup>, H.-F. Wirth <sup>a</sup>, O. Zimmer <sup>a</sup>

<sup>a</sup>Physik-Department E18, TU München, James-Franck-Straße, 85748 Garching, Germany

<sup>b</sup>Physik-Department E21, TU München, James-Franck-Straße, 85748 Garching, Germany

<sup>c</sup>PN Sensor GmbH, Römerstraße 28, 80803 München, Germany

<sup>d</sup>Max-Planck-Institut für extraterrestrische Physik, Giessenbachstraße, 85741 Garching, Germany

<sup>e</sup>MPI Halbleiterlabor, Otto-Hahn-Ring 6, 81739 München, Germany

---

## Abstract

The detection of low-energy protons is a well known problem in various neutron decay studies. We report first measurements with a silicon drift diode (SDD) using protons with impact energies in the range from 10 keV to 16 keV. Compared to a standard PIN diode the SDD shows a much improved separation of the proton signal from noise. This detector type initially developed for X-ray spectroscopy will therefore become very useful for proton detection in forthcoming neutron decay experiments. It might also be applied in other projects involving low-energy charged particle detection.

*Key words:* SDD, protons, neutron physics

*PACS:* 29.40.Wk, 07.77.Ka, 23.40.-s

---

## 1. Introduction

The decay of the free neutron,  $n \rightarrow p + e + \bar{\nu}_e$ , offers a variety of observables important for the accurate determination of semi-leptonic weak interaction parameters, as well as many tests of the standard model of particle physics at the low-energy frontier. Many studies involve the detection of protons, emitted with a maximum recoil energy of only 751 eV. To obtain a signal well separated from noise, decay protons are usually accelerated onto the detector by at least 25 kV. Such high voltages have frequently caused electrical stability problems, in particular if the experiment involves strong magnetic fields.

We first mention some projects in neutron decay which might benefit from proton detection with a lower acceleration voltage. In a recent first observation of the radiative decay mode of the free neutron [1], a surface barrier detector was employed for proton detection, using a coincidence technique to observe low-energy  $\gamma$  quanta emitted together with the normal decay products. The same detector was previously employed in several experiments on

the neutron lifetime, for counting decay protons stored in a Penning trap [2, 3]. A new neutron lifetime experiment employing ultracold neutrons with proton detection is in preparation [4]. The latest, most accurate experiments to determine a time reversal invariance violating phase between vector- and axial-vector currents in neutron decay measured a triple correlation between neutron spin and the momenta of electron and proton. In both experiments, named TRINE and emiT, protons were detected by arrays of PIN diodes [5–7]. The project which has triggered the present study is a measurement of the integral proton recoil spectrum in free neutron decay to provide a very accurate value of the axial-vector-to-vector ratio of the weak coupling constants. The spectrometer *a*SPECT [8, 9], developed in collaboration with a group from Mainz University, involves detection of protons in presence of a several Tesla strong magnetic field. First experiments at the Munich research reactor FRM-II were performed with a segmented silicon PIN diode with 25 strips with size 25 mm  $\times$  0.8 mm each, set at a potential of about  $-30$  kV. Even with this high acceleration potential, the proton peak was hardly separated from the noise of the system. Similar noise characteristics were found using our laboratory proton source with the detector at ground potential (see Fig. 2). Repeated electrical breakdown during further beamtimes motivated

---

\* Corresponding author. Tel.: +49-89-289-12379; Fax: +49-89-289-12570.

*Email address:* msimson@e18.physik.tu-muenchen.de (M. Simson).

the search for a better solution.

We considered a silicon drift diode (SDD) as a promising device for low-energy proton detection. It has been developed mainly to measure X-ray radiation, especially in X-Ray Fluorescence (XRF) applications.

## 2. The silicon drift detector

The silicon drift detector principle was first proposed by E. Gatti and P. Rehak in 1984 [10]. It is based on the side-ward depletion principle which allows the full depletion of a large detector volume with a very small readout node. Hence, the thermal noise which is proportional to the total anode capacitance is greatly reduced when compared to a conventional PIN diode whose capacitance increases linearly with the active area.

A further improvement of the detector noise performances is achieved by integrating the first amplification FET directly onto the detector bulk (see Fig. 3). This minimizes stray capacitances and eliminates the pick-up noise and microphony effects related to wire connections between the detector anode and the front-end electronics. Signal-charge, i.e. electrons generated by any ionizing particle in the detector bulk, drifts in an electric field toward the small readout anode situated in the detector center, where it is amplified by the integrated FET. Further details on SDDs and their applications can be found in Refs. [11, 12].

For the tests presented here, a detector manufactured by the MPI Halbleiterlabor [13] in cooperation with PNSensor GmbH [14] was used. The detector has an active volume of  $30 \text{ mm}^2 \times 450 \text{ }\mu\text{m}$  with a homogeneous thin entrance window covered by 30 nm aluminum. The detector chip is mounted on a Peltier cooler inside a small housing with an external collimator ring. The temperature of the SDD chip is monitored by an integrated temperature diode.

The signal charge collected at the detector anode is amplified by a charge sensitive amplifier [15]. The amplifier output signal is processed by a semi-Gaussian shaper with a shaping time of 1  $\mu\text{s}$  (peaking time 2.5  $\mu\text{s}$ ) and digitized by an analog to digital converter. Since there is no external trigger, the digitized signals are continuously sampled by field programmable gate arrays (FPGAs) and analyzed with respect to a triggering algorithm comparing the level of the baseline to the signal height. When a trigger decision is made, an event with a length of 10  $\mu\text{s}$  is sent to a personal computer where it is stored for offline analysis of the data.

## 3. Spectroscopic investigations of the detector

The basic output of the electronics is a pulseheight proportional to the energy deposited in the active volume of the detector. To convert this pulseheight into the energies given in the figures, Gaussian peaks were fitted for the  $K_\alpha$  and the  $K_\beta$  line of manganese. The well known energies (5.90 keV and 6.49 keV for  $K_\alpha$  and  $K_\beta$  [16]) of these lines provide a linear calibration of the detector. Full agreement

was obtained in a cross check of this calibration curve using the position of the  $K_\alpha$  escape peak (4.16 keV [17]). The energy calibration obtained from these lines is shown on the top axes of Figs. 4-6. This calibration is not valid for Fig. 2, since different front-end electronics is used for the segmented PIN diode.

The effect of cooling the detector with the Peltier element is visible in Fig. 4. Lowering the temperature significantly improves the resolution. At about  $-13\text{C}$ , the full width at half maximum of the  $K_\alpha$  line of manganese is about 164 eV. Under optimized conditions, values below 140 eV are possible with this detector. At this temperature hardly any noise can be seen above 0.2 keV.

In contrast to X-ray photons, massive charged particles with energies of several keV penetrate solid material only to a depth of few hundred nanometers. Along their path to the active volume of the detector they lose a part of their energy due to ionisation in the entrance window, which therefore has to be as thin as possible. As a statistical process this energy loss results in broadening of the detected peak (called straggling) and deviation from Gaussian shape.

To investigate the properties of the detector we used a laboratory source of low-energy protons produced from hydrogen gas ( $\text{H}_2$ ) by an extractor type ion source. The source is held at high potential for particle acceleration. A 30 bending magnet is used as mass separator. Furthermore, a three-element Einzel lens [18] and two irises with 2 to 40 mm aperture are available for beam definition. This so-called “proton accelerator with femto ampere flux” (paff) [19] allows us to produce protons with energies between 10 and 35 keV with an adjustable flux ranging from several  $\mu\text{A}$  down to several protons per second.

In a first test, the detector was held at room temperature (24C) and irradiated with protons having impact energies between 10 keV and 16 keV. The results are shown in Fig. 5. The beam intensity is strongly dependent on the acceleration voltage and the field of the bending magnet. Since these parameters have to be changed for every impact energy, the various proton spectra shown in Fig. 5 differ in height. The intensity with pulseheights below 200 ADC channels is the thermal noise of the system. This peak persists when the proton beam is off, as visible in Fig. 6.

The detected energy corresponding to the gamma-calibration is about 5.2 keV, 5.7 keV, and 6.1 keV less than the proton impact energies 10 keV, 12 keV, and 14 keV respectively, due to the detector entrance window and the different ionisation pattern of protons compared to x-rays. The full width at half maximum is roughly the same for all energies at about 1 keV. These values meet the expectation and are consistent with our simulations<sup>1</sup>.

When the detector is held at low temperature the proton spectrum changes with time. The peak center stays at the same position but a shoulder develops at the low-energy side. Whereas the peak is getting smaller, the total count rate remains almost constant. A possible reason for this be-

<sup>1</sup> Simulations have been done with the program SRIM [20].

havior might be water contained in the rest gas condensing on parts of the cold detector surface.

#### 4. Conclusion and outlook

The present study shows that silicon drift detectors offer significant advantages for low-energy proton detection compared to standard PIN diodes. The small readout anode of the SDD combined with the first amplification stage implemented on the detector chip results in excellent noise characteristics. As an important benefit for detection of protons from neutron decay, a much lower acceleration potential will be needed for a sufficient separation of the signal from noise. Although the tested detector was rather small, similar results are expected for larger detectors since proton straggling dominates the noise performance and an additional leakage current contribution due to the larger volume is negligible.

Further investigations on SDDs with low-energy protons will be performed with the cooled detector protected by a cryogenic shield to avoid condensation of moisture on the detector surface. Furthermore, the effect of different entrance window types will be studied.

#### References

- [1] J. S. Nico et al., *Nature* **444** (2006) 1059.
- [2] J. Byrne et al., *Phys. Rev. Lett.* **65** (1990) 289.
- [3] M. S. Dewey et al., *Phys. Rev. Lett.* **91** (2003) 152302.
- [4] R. Picker et al., *J. Res. Natl. Inst. Stand. Technol.* **110** (2005) 357.
- [5] T. Soldner et al., *Phys. Lett. B* **581** (2004) 49.
- [6] T. Soldner et al., *Nucl. Instr. and Meth. A* **440** (2000) 643.
- [7] L.J. Lising et al., *Phys. Rev. C* **62** (2000) 055501.
- [8] O. Zimmer et al., *Nucl. Instr. and Meth. A* **440** (2000) 548.
- [9] F. Glück et al., *Europhys. Journal A* **23** (2005) 135.
- [10] E. Gatti and P. Rehak, *Nucl. Instr. and Meth. A* **226** (1984) 608.
- [11] G. Lutz, *Semiconductor Radiation Detectors*. Springer, Berlin, Heidelberg, New York, 1<sup>st</sup> edition, 1999.
- [12] A. Niculae et al., *Nucl. Instr. and Meth. A* **568** (2006) 336.
- [13] Semiconductor Laboratory (Halbleiterlabor in German) of the Max-Planck-Institut für Physik and the Max-Planck-Institut für extraterrestrische Physik, <http://www.hll.mpg.de>.
- [14] PNSensor GmbH, <http://www.pnsensor.de>.
- [15] C. Fiorini, *Nucl. Instr. and Meth. A* **568** (2006) 106.
- [16] G. Hölzer et al., *Phys. Rev. A* **56** (1997) 4554.
- [17] S. J. B. Reed and N. G. Ware, *J. Phys. E* **5** (1972) 582.
- [18] E. Harting and F. H. Read, *Electrostatic lenses*. Elsevier, Amsterdam, 1976.
- [19] A. R. Müller et al., to be submitted to *Nucl. Instr. and Meth. A*.
- [20] J. F. Ziegler et al., SRIM - The Stopping and Range of Ions in Matter. Computer Program. <http://www.srim.org> (2006).

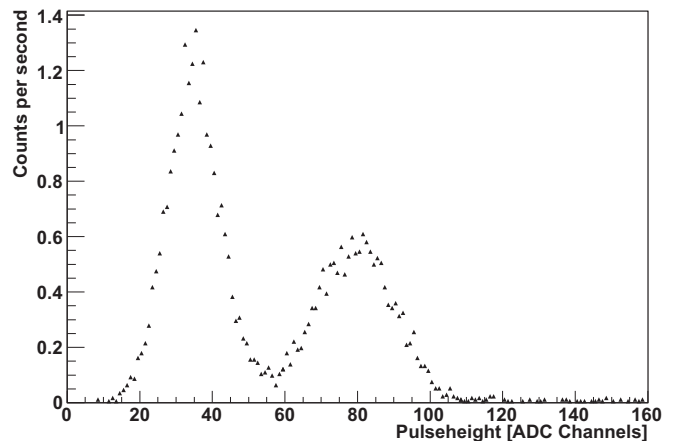


Figure 1. Proton pulseheight spectrum taken with one strip of the segmented silicon PIN diode. The electronic noise (left peak) is hardly separated from the proton signals (right). This spectrum was taken with 30 keV protons from our laboratory source.

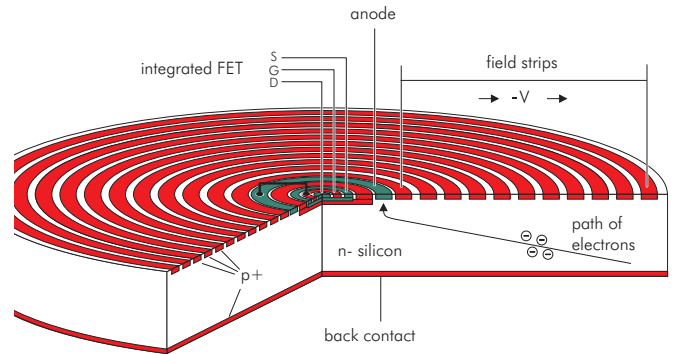


Figure 2. Schematic cross section of a SDD. Signal charges (electrons) are created by ionizing particles and drift towards a central ring-shaped anode. The anode is connected to the gate of an integrated FET, which acts as a first amplification stage. Radiation enters the detector through the back contact.

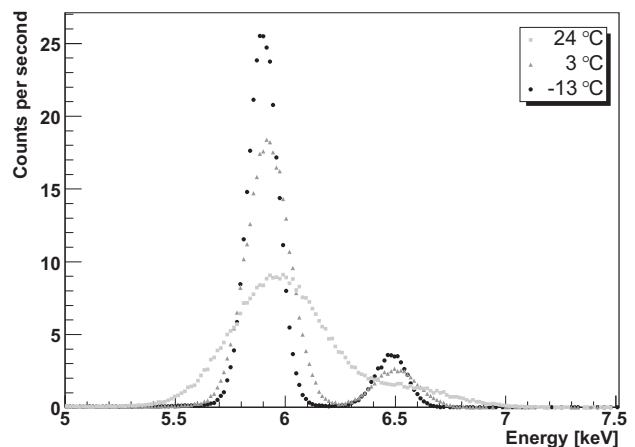


Figure 3. The manganese  $K_{\alpha}$  and  $K_{\beta}$  lines following the  $\beta$  decay of a  $^{55}\text{Fe}$  calibration source, measured for different temperatures of the detector. The energy resolution at 24C is reduced due to the non-optimized shaping time for this temperature.

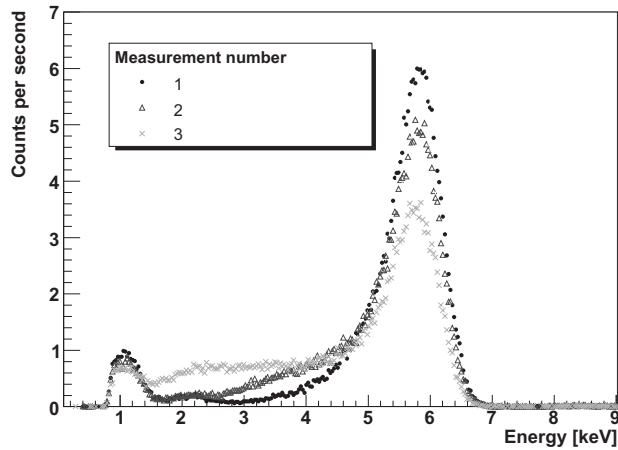


Figure 4. Proton pulseheight spectra for different proton impact energies, taken with the detector at room temperature. The peak at low energies is the thermal noise of the detector and the electronics. For 16 keV protons, events with too high amplitudes are cut off, because the maximum amplification of the preamplifier/shaper used is reached. The small peak at about 2 keV is caused by secondary electrons. They are produced when protons hit the apertures of the accelerator.

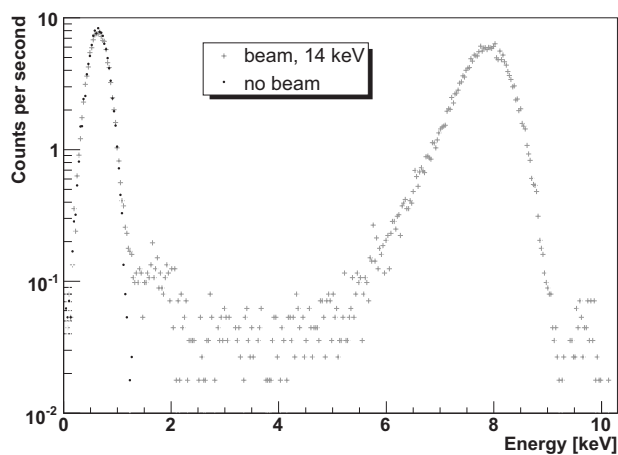


Figure 5. A spectrum with the proton beam set to 14 keV impact energy compared to a spectrum where the beam is blocked by a vacuum shutter.